AN EXPERIMENTAL INVESTIGATION OF HEAT TRANSFER RATES ON A BLUNT BODY IN HYPERSONIC FLOW

Thesis by

Homer K. Richards, Jr.

Lieutenant, U. S. Navy

In Partial Fulfillment of the Requirements

For the Degree of

Aeronautical Engineer

California Institute of Technology

Pasadena, California

1957

ACKNOWLEDGMENTS

The author wishes to express his gratitude and appreciation to Professor Lester Lees for his supervision and encouragement throughout the course of this investigation.

He further wishes to express his appreciation to Mr. F. W. Hartwig, who, despite his own heavy schedule, was always available for consultation and advice on all phases of the project.

Mr. C. A. Bartsch and his co-workers at the GALCIT machine shop contributed heavily toward the success of this endeavor. The author is particularly indebted to Mr. George Carlson for the fabrication of the models and to Mr. H. McDonald for the tedious tasks of constructing, installing and maintaining the heat meters and thermocouples used in this study.

Appreciation is expressed to Mr. Paul Baloga and the staff of the GALCIT 5 x 5 inch hypersonic wind tunnel for their contribution. Mr. Sam Roman of this staff provided many valuable suggestions concerning tunnel installations and techniques.

The writer finally wishes to thank Mrs. G. Van Gieson for her excellent preparation of the manuscript.

ABSTRACT

An experimental investigation was made in the GALCIT hypersonic wind tunnel, leg number 1, at a nominal Mach number of 5.8 to determine the heat transfer rate and temperature distributions on a water-cooled, ellipsoid-cone at angles of yaw of 0, 4 and 8 degrees, respectively. The Reynolds number per inch based on free stream conditions was 2.03×10^5.

The experimental means employed was a steady-state technique developed by Mr. F. W. Hartwig at GALCIT during the past several years. This technique utilizes a heat transducer or heat meter of very small size. The primary advantage of this method is that it obviates the necessity of correcting for axial temperature gradients in the model.

Surface pressure distributions were also studied on a model of identical geometry for angles of yaw of 0, 4, 8 and 12 degrees, respectively. The primary interest here was to obtain data necessary for the theoretical calculation of the heat transfer rate distributions using laminar flow theory.

The investigation showed that the heat meters were very reliable. The data obtained from independent wind tunnel runs were repeatable within $\pm$ 1.5 per cent. It was found that the local heat transfer rate and the local pressure coefficient vary linearly with angle of yaw. The agreement of the experimentally determined stagnation heat transfer rate and the theoretically calculated one was good. Further refinement of the calibration technique appears to be the logical direction of effort for subsequent investigators.

TABLE OF CONTENTS

LIST OF FIGURES

LIST OF SYMBOLS

C_p	local pressure coefficient, $(p - p_\infty)/(\frac{1}{2} \rho_\infty u_\infty^2)$
$C_{p_{max}}$	pressure coefficient at the stagnation point
D	cone base diameter
p	static pressure
$\dot{q}_w$	local heat transfer rate
$\dot{q}_{w_o}$	heat transfer rate at the stagnation point
R_o	radius of curvature at the nose
U	velocity
x, y, z	a right hand coordinate system, fixed in the body with the x- axis along the model longitudinal axis
α	angle of yaw
δ	shock wave stand-off distance at the stagnation point at zero angle of yaw
ρ	density
$( )_w$	surface conditions
$( )_\infty$	free stream conditions

I. INTRODUCTION

The problem of heat transfer and its experimental determination in hypersonic flow has become an increasingly important one in the past several years, as flight speeds have steadily increased.

Many problems have arisen in the experimental techniques employed. Any attempt at steady-state heat transfer measurements has been plagued by the necessity of correcting for axial temperature gradients in the material used. These corrections are often of the same order as the measured values, with a subsequent excellent possibility of large experimental errors and poor repeatability.

To alleviate this problem, Mr. F. W. Hartwig (Ref. 1) has developed a steady-state technique utilizing a heat transducer or heat meter of very small size. His results have been very encouraging and further use of the method was definitely indicated.

The model configuration studied in this investigation was a body of revolution with ellipsoidal nose and conical afterbody. The two portions were joined by a fairing so that no discontinuity in the radius of curvature existed. Two models of identical geometry were used, one for the determination of surface pressure distributions, the other for determining heat transfer rates and temperature distributions. The pressure model was studied at angles of yaw of 0°, 4°, 8° and 12°. The heat model investigation was limited to angles of yaw of 0°, 4° and 8°.

The work was performed in the GALCIT 5 x 5 inch hypersonic wind tunnel at a nominal Mach number of 5.8 and at a Re/in. of 2.03×10^{5} based on reservoir conditions.

II. EXPERIMENTAL EQUIPMENT AND PROCEDURE

A. Description of the Wind Tunnel and Instrumentation

The experimental testing was performed in the GALCIT 5" x 5" hypersonic wind tunnel (leg no. 1), which is a continuous flow, closed-return type. The compression ratios required were obtained with five stages of Fuller rotary compressors, (Fig 1). All controls were operated from a master control panel adjacent to the test section. The air heating system consisted of a multiple-pass heat exchanger with superheated steam as the heating medium. Limits of system capacity were 275^{o}F. at a stagnation pressure of 74 psig.

The air was dried by a 2200 pound bed of silica gel in the main air circuit. The silica gel was reactivated by an integral blower-heater-condenser.

The nominal Mach number in the test section was 5.8. The Foelsch method was used to design the nozzle blocks. Corrections were made to account for estimated boundary layer displacement thickness. Nozzle calibration was checked by static orifices in both the top and bottom nozzle blocks. The test section with model mounting is shown in Fig. 2.

Two vacuum-references manometers were used to measure model static pressures, one using DC-200 silicone fluid and the other using mercury. Tunnel stagnation pressure was measured with a Tate-Emery, nitrogen-balanced gage and this pressure was controlled within $\pm$ .04 psi by means of a Minneapolis-Honeywell-Brown circular chart controller.

Tunnel stagnation temperature was controlled by means of a

Minneapolis-Honeywell-Brown circular chart controller within $\pm$ 2°F. The reference stagnation temperature was obtained by a thermocouple probe located one inch upstream from the nozzle throat.

A 24 channel Minneapolis-Honeywell-Brown potentiometer pyrometer was used to obtain thermocouple and "heat meter" outputs from the heat model.

Schlieren photographs of the flow were made by using an optical system using a BH-6 steady source.

B. Description of the Models

Two models of identical geometry were used during this investigation. The configuration was an ellipsoid-cone with a fairing between the two portions so that no discontinuities in the radius of curvature existed. One model was used to obtain pressure distributions and the other to obtain heat transfer and temperature distributions for the various angles of yaw. Fig. 3 is a photograph of the heat model showing the heat meters and associated painted circuitry.

The pressure model was constructed of brass with twelve conventional static pressure orifices of .016 inch diameter. Fig. 4 shows the internal construction of the model. The orifices were located on four radials and are identified by number as indicated in Fig. 7. The semi-vertex angle of the conical portion was 10° and the base diameter was 1.5 inches.

The equation of the ellipsoidal nose portion of the model is

$$\frac{(x - .375)^2}{(.375)^2} + \frac{y^2}{(.550)^2} + \frac{z^2}{(.550)^2} = 1 \quad ,$$

where the coordinate system origin is taken as the apex of the nose. The major axis is perpendicular

to the longitudinal axis of the model.

The heat model was constructed of rolled steel with a wall thickness of .050 inches. The model was coated with a .020" porcelain layer which served a dual purpose. It provided an insulator for the heat meters and the painted circuits and it increased meter sensitivity as compared to meter installations in the steel wall itself, because of the low thermal conductivity of the procelain.

The model was cooled by water conveyed through coaxial tubing, which also served as the sting support when the model was installed in the wind tunnel. Fig. 5 illustrates the internal construction of the heat model. The water flow was approximately fifteen gallons per hour. This flow rate provided sufficient cooling to maintain the temperature differential between the incoming and outgoing coolant at less than 1^{o}F. under tunnel conditions and less than 2^{o}F. when calibrating.

The heat meter is essentially a thermopile on a miniature scale. Fifty turns of one mil constantan wire spaced .001" apart were wound on a glass core .007" x 1/16" x 1/8". One-half of each loop was then silver-plated, resulting in silver-constantan junctions with a thermocouple spacing of .007". For protection and to prevent shorting, a thin coat of Adweld was applied to the finished meter. Refs. 1 and 2 are a source of more information on their construction and appearance.

Installation of the heat meter in the model surface was accomplished by grinding a small indentation in the ceramic coating and cementing the meter in place. The meter was connected to silver-plated turret posts cemented in a micarta insulation ring on the base of the model by means of painted silver circuits. Nine heat meters were installed in the model used in this experiment (Fig. 7).

Surface temperature distributions were obtained from a line of ten thermocouples installed on the surface of the model. The thermocouples were formed by cementing a one mil constantan wire on the model and making contact with this wire at ten points with silver paint. As in the case of the heat meters, the painted portion of the circuit terminated at turret posts on the base of the model.

One constantan and twenty-two silver leads were soldered to the turret posts at the base of the model to provide connections to the Minneapolis-Honeywell-Brown potentiometer pyrometer. Silver leads were used to eliminate the possibility of erroneous thermoelectric effects induced due to temperature differences at the turret posts.

C. Model Mounting

The models were mounted in the portion of the test section with most uniform flow conditions as determined by earlier static pressure calibration surveys.

Both models were sting supported and the sting was mounted on two vertically actuated struts, 3.825 inches apart. These struts were driven by a small electric motor and their vertical position could be determined to within .001 inch accuracy. Differential movement of the struts provided for the setting of desired angles of yaw.

Two methods of obtaining the desired rotational positions were used, one for the pressure model and a second for the heat model.

The sting support for the pressure model had a machined collar and shaft arrangement that permitted rotation to any position about the longitudinal axis. A set screw in the collar locked the model at the

desired setting.

The heat model was positioned by means of external collars fitting over the sting. These collars had threaded holes on 45^{o} centers. Thus, eight rotational positions were provided for and were determined very accurately by the machining of the collar. Allen-head screws were used to attach these collars to special supports in such a way that the sting was free to rotate about an axis perpendicular to the plane of the supports. The supports were in turn attached to the vertical struts. One collar was fixed to the sting and the other was free to slide so that the angle of yaw could be changed at will.

Saran tubing was used to connect the steel tubes at the base of the pressure model to external leads going to the manometer boards. Tygon tubing conveyed the coolant to the base of the coaxial sting in the case of the heat model.

D. Heat Meter Calibration

The calibration technique was one of exposing the model to a known input of power and recording the electrical output of the heat meters. This output was then converted to terms of heat flow ($BTU/ft^2/hr$). It is of the utmost importance that the model be exposed to a uniform heat source and that the surface temperature distribution be uniform. Only if these two conditions are essentially met, can any accurate calibration be accomplished.

It was also apparent that heat losses in the calibrating heater would have to either be accounted for or virtually eliminated. At first, attempts were made to measure the losses accurately by the use of commercial heat meters. These early tests indicated that for

a given heat input the losses were of the same order as the heat passing through the model. Any error in the loss measurement would be reflected as an error of the same magnitude when considering heat input through the model. This author felt that sufficient accuracy under the early experimental set-ups was not attainable. Another disadvantage of this first system was the long periods of time required before equilibrium was reached because of the heavy insulation used to reduce external heat losses.

The second method, that of virtually eliminating losses, was accomplished in the following manner (Fig. 6): A heater was built that conformed to the model shape and allowed a uniform 3/16" air gap between the model and the heater elements. A long, flexible heat meter was constructed of .008 constantan wire wrapped on a thin strip of mica, then silver-plated in the usual manner. This heat meter was wrapped around the calibration heater. A second heater was built around the first with a spacing of approximately 1/8 inch. Its function was to act as a bucking heater. During calibration runs when the heat meter was "nulled" there was no heat flow outward from the model heater element and, therefore, no heat losses. It is estimated that the losses were held to $\pm$ 2 per cent of the heat input to the model. This estimate is based on the sensitivity of the null heat meter and the magnitude of the changes in power to the bucking heater required for "nulling". A further advantage of this system was the marked shortening of the time required for equilibrium because the need for external insulation no longer existed. To prevent losses out of the base of the model, a circular heat meter and bucking heater were used in an analogous manner.

Readings were taken in several rotational positions to reduce errors introduced by positioning and non-uniform heat source. The maximum spread in calibration data from this source was $\pm$ 7 per cent. The calibration curve for a typical heat meter is presented in Fig. 8.

E. Thermocouple Calibration

The calibration for a silver-constantan thermocouple is presented in Fig. 9. This calibration was previously performed in connection with the investigation of Ref. 1.

F. Test Procedure

1. Surface Pressure Data

Upon installation in the test section, the system was thoroughly leak-checked. Ample time was allowed for temperature stabilization of the test section, etc., before any data were taken.

To minimize flow irregularities across the test section, the model was rotated about its longitudinal axis in five different positions 45 degrees apart. In each rotational position, the model was yawed twelve degrees above and below the horizontal in 4 degree increments. This procedure yielded complete pressure surveys for the vertical, horizontal and two diagonal meridian planes.

All tests were made at a reservoir stagnation temperature and pressure equal to 270^{o}F. and 88.5 psia, respectively. The Reynolds number per inch based on free stream conditions was 203,000. At this Re it was assured that the experiment was carried out in the laminar boundary layer regime.

2. Heat Transfer Data

Tunnel conditions were identical to those used in the pressure tests. The maximum angle of yaw attainable was reduced to 8 degrees. This limitation was caused by a protrusion of the sting downstream of the rear support of about one inch, which served as a connecting link to the coaxial tubing. When angles of yaw were introduced, this protrusion made contact with the tunnel walls and limited the angle of yaw. The rotational procedures were repeated as before and heat transfer data in four meridian planes was recorded.

Three complete sets of data were taken in this case to check the repeatability of the heat meters. Each set of data was evaluated and then compared, meter by meter. The maximum deviation from the mean of the three values at each meter was $\pm$ 1.5 per cent. In most cases it was less than $\pm$ .5 per cent. In view of this fact, these three sets of values were averaged and plotted as single experimental points when the data were presented in graphical form.

3. Temperature Data

The temperature distributions were obtained in a completely analogous manner. Because of model construction difficulties, the line of thermocouples was not aligned with any given plane of heat meters and a completely separate set of runs was required.

III. DISCUSSION OF RESULTS

A. Schlieren Observations

Figures 10 through 13 are schlieren photographs of the pressure model at angles of yaw of 0, 4, 8 and 12 degrees. Schlierens of the heat model were omitted since there was nothing of interest to be noted.

It is evident that the shape of the bow shock wave is dominated by the geometry of the elliptical portion of the model. This phenomenon is discussed by Lees and Kubota (Ref. 3) and is caused by the fact that in hypersonic flow, the drag/area of the blunt-nose is much greater than the drag/area of an afterbody with a uniformly small slope. It is interesting to note that the distortion to the shock wave, caused by the angle of yaw of the model, is small in relation to the fixed tunnel coordinates.

The ratio of the detachment distance, δ, between the bow shock wave and body surface on the longitudinal axis at zero angle of yaw, to the nose radius, R_o, at this point was found to be .127. This compares to theoretically predicted values of 0.118 by Hayes (Ref. 4) and 0.137 by Ting-Yi Li (Ref. 5) for spherical-nosed bodies of revolution at M = 5.8.

B. Surface Pressure Distributions

The experimental surface pressure distributions are presented in Figs. 14 through 17, in terms of $C_p/C_{p_{max}}$ versus S/D, where S is measured along the body surface from the apex and D is the base diameter.

For comparison, theoretical distributions based on the modified Newtonian approximation are also plotted on Figs. 14 and 17. The experimental values fall somewhat below those predicted in the region of most rapidly changing pressure. On the conical portion $C_p/C_{p_{max}}$ is somewhat higher than the Newtonian. This behavior is anticipated because for small cone half angles, the nose drag dominates the flow pattern several nose diameters downstream on the conical skirt. This effect has been noted experimentally many times, see for example O'Bryant (Ref. 6).

The angle of yaw data is presented for two meridian planes, the vertical plane and the diagonal inclined 45 degrees to the vertical. The diagonal plane values represent an average of the two diagonal planes since data differed by less than 2 per cent.

Data were also taken in the horizontal plane, but they were not presented graphically, because the change in $C_p/C_{p_{max}}$ from the zero angle of yaw case for any given surface position was less than four per cent for the extreme cases of 12 degree yaw angle. This behavior is explained by the fact that the effective change in the angle of yaw of the horizontal plane is much less than that experienced by the vertical and diagonal planes.

As has been pointed out in Ref. 6, it appears that the change in the ratio $C_p/C_{p_{max}}$ with angle of yaw for a given position on the model is essentially linear over the range of yaw angles studied ($\pm$ 12°).

C. Heat Transfer Rate Distribution

The experimental heat transfer rate distributions are presented in Figs. 18 and 19. They are plotted in terms of non-dimensional

quantities $\dot{q}_w/\dot{q}_{w_o}$ versus S/D where $\dot{q}_w$ is the local heat transfer rate and $\dot{q}_{w_o}$ is the heat transfer rate at the stagnation point.

As in the case of the pressure distribution curves, the results are presented in the vertical and diagonal meridian planes. The horizontal plane was again omitted because the changes in the heat transfer rates from the zero angle of yaw case were less than four per cent for reasons previously stated.

Experimentally, the stagnation heat transfer rate was determined to be 8560 BTU/hr/ft^2. Theoretical calculations for the stagnation point heat transfer rate, according to Lees (Ref. 7), yielded a stagnation value of 8460 BTU/hr/ft^2. Calculation according to Reshotko and Cohen (Ref. 8) yielded a stagnation value of 8760 BTU/hr/ft^2. The experimental value found is 2.3 per cent lower than the latter value and 1.2 per cent higher than that predicted by the use of the Lees paper. This result is considered by the author to represent excellent agreement for heat transfer work.

Figs. 18 and 19 show that apparently the local heat transfer rates vary linearly with angle of yaw for the angles used in this experiment. This observation applies not only to the vertical meridian plane, but also to the diagonal meridian plane, where the heat transfer rates are influenced by many different streamlines.

Fig. 18 indicates that the stagnation heat transfer rate was not reached at any point in the vertical plane for the 8^o angle of yaw case. It is a matter of only 2 per cent but some comment on this point is warranted. This apparent inconsistency could be caused either by experimental errors, or by a change in the stagnation heat transfer rate. The latter possibility cannot be discounted since the

velocity gradient, $(du/ds)_o$, depends on the body radius of curvature and changes with yaw angle. A further point to consider is that the pressure distribution, near the stagnation point, at 8^o angle of yaw lies somewhat above that predicted by modified Newtonian theory (Fig. 16).

D. Surface Temperature Distributions

Figs. 20 and 21 contain the experimental surface temperature distributions for the vertical and diagonal meridian planes at angles of yaw of 0, 4 and 8 degrees respectively.

The inflection point in each of the temperature curves near the ellipse-cone junction has moved back on the model to a position where the value of S/D is approximately .52 as compared to .42 for the pressure or the heat case. This effect is attributed to the presence of axial heat conduction in the metal shell of the model. This shift would cause no difficulty when theoretical and experimental heat transfer distributions are compared since the empirical temperature distributions are used to calculate the theoretical heat transfer rates.

IV. CONCLUSIONS

The following conclusions can be drawn from this investigation in the GALCIT 5" x 5" hypersonic wind tunnel (leg no. 1):

1. The steady-state technique used in this investigation yielded excellent results under the present test conditions.

2. The maximum deviation of a given heat meter output for three separate sets of wind tunnel data was 1.5 per cent.

3. The maximum scatter in calibration data points because of positioning or uneven heat sources was $\pm$ 7 per cent.

4. The agreement of the experimentally determined stagnation heat transfer rate and the theoretically calculated one was good.

5. The local heat transfer varies linearly with angle of yaw over the range tested.

6. The surface pressure distribution over the elliptical-nose agrees very closely to that predicted by the modified Newtonian theory.

7. The local pressure coefficient varies linearly with angle of yaw up to 12 degrees.

8. Subsequent investigators should concentrate their attention to refining the calibration technique in an effort to reduce the $\pm$ 7 per cent spread in this data.

9. The heat meters themselves need no refinement and meter configuration changes should be attempted only if application demands it.

REFERENCES

1. Hartwig, F. W.: Development and Application of a Technique for Steady-State Aerodynamic Heat Transfer. GALCIT Hypersonic Research Project, Memorandum No. 37, June 1, 1957.

2. Hartwig, F. W.; Bartsch, C. A.; and McDonald, H.: Miniaturized Heat Meter for Steady-State Aerodynamic Heat-Transfer Measurements. Journal of the Aeronautical Sciences, Vol. 24, No. 3, p. 239, March, 1957.

3. Lees, Lester and Kubota, Toshi: Inviscid Hypersonic Flow over Blunt-Nosed Slender Bodies. Journal of the Aeronautical Sciences, Vol. 24, No. 3, pp. 195-202, March, 1957.

4. Hayes, W. D.: Some Aspects of Hypersonic Flow. Ramo-Wooldridge Corporation, January, 1955.

5. Li, Ting-Yi and Geiger, R. E.: Stagnation Point of a Blunt Body in Hypersonic Flow. Institute of the Aeronautical Sciences, Preprint No. 629, January, 1956.

6. O'Bryant, William T.: An Experimental Investigation of Hypersonic Flow over Blunt-Nosed Cones at Mach Number of 5.8. GALCIT Hypersonic Research Project, Memorandum No. 32, June 15, 1956.

7. Lees, Lester: Laminar Heat Transfer over Blunt-Nosed Bodies at Hypersonic Flight Speeds. Jet Propulsion, Vol. 26, pp. 259-269, April, 1956.

8. Cohen, C. B. and Reshotko, E.: Heat Transfer at the Forward Stagnation Point of Blunt Bodies. NACA TN 3513, 1955.

9. Ames Research Staff: Equations, Tables, and Charts for Compressible Flow. NACA Technical Report 1135, 1953.

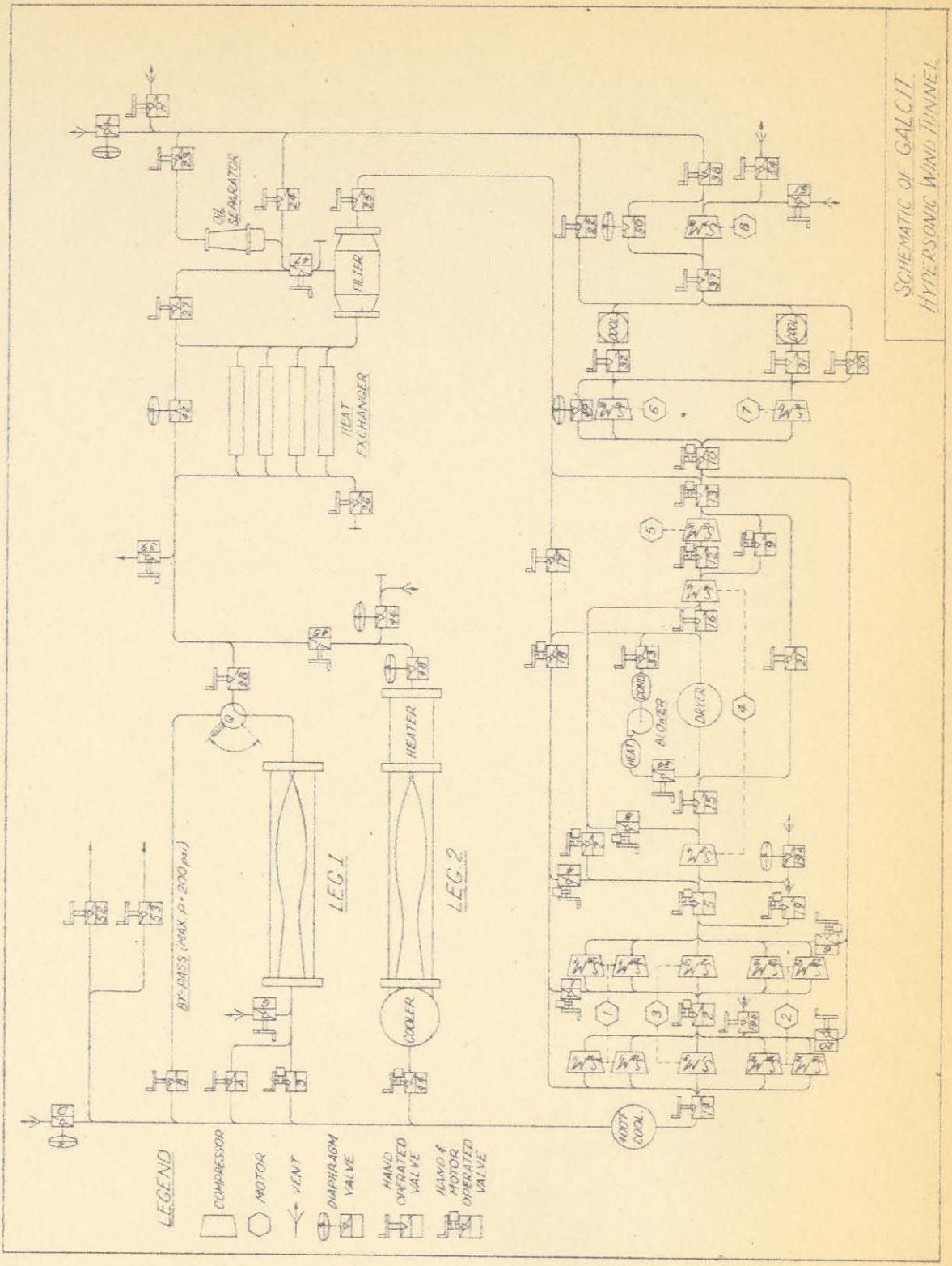
SCHEMATIC OF GALCIT
HYPERSONIC WIND TUNNEL
OIL SEPARATOR
FILTER
HEAT EXCHANGER
HEATER
COOLER
LEG 1
LEG 2
BY-PASS (MAX. P = 200 psi)
DRYER
HEAT
COND.
BLOWER
ADDT. COOL.
LEGEND
COMPRESSOR
MOTOR
VENT
DIAPHRAGM VALVE
HAND OPERATED VALVE
HAND & MOTOR OPERATED VALVE

FIG. 1

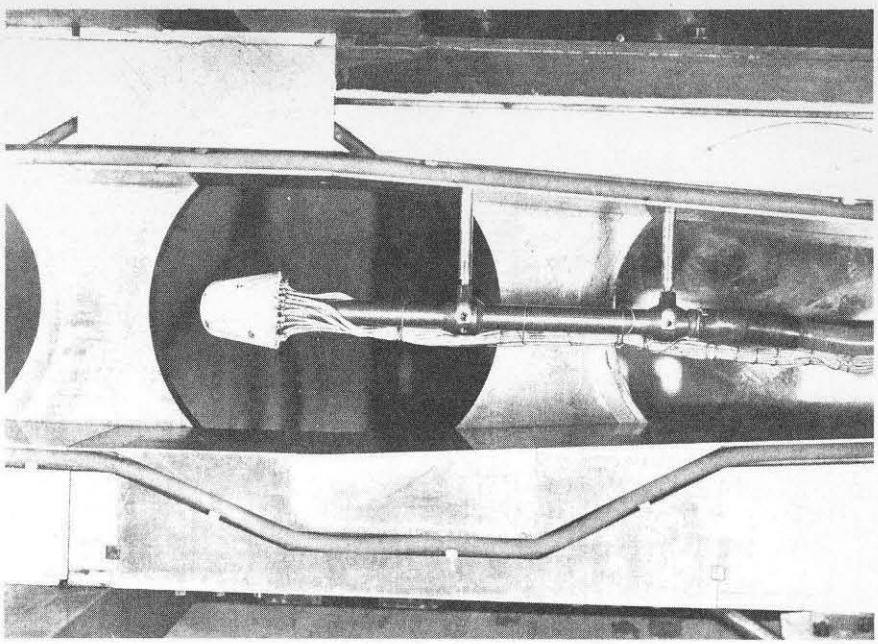

FIG. 2

TEST SECTION OF HYPERSONIC TUNNEL

SHOWING METHOD OF MOUNTING MODEL

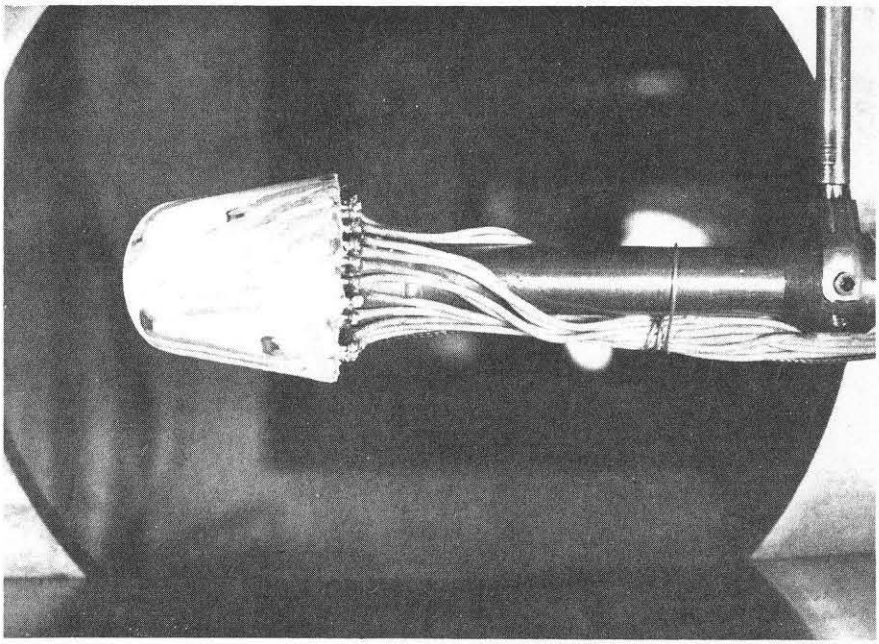

FIG. 3

HEAT MODEL SHOWING HEAT METERS AND PAINTED CIRCUITS

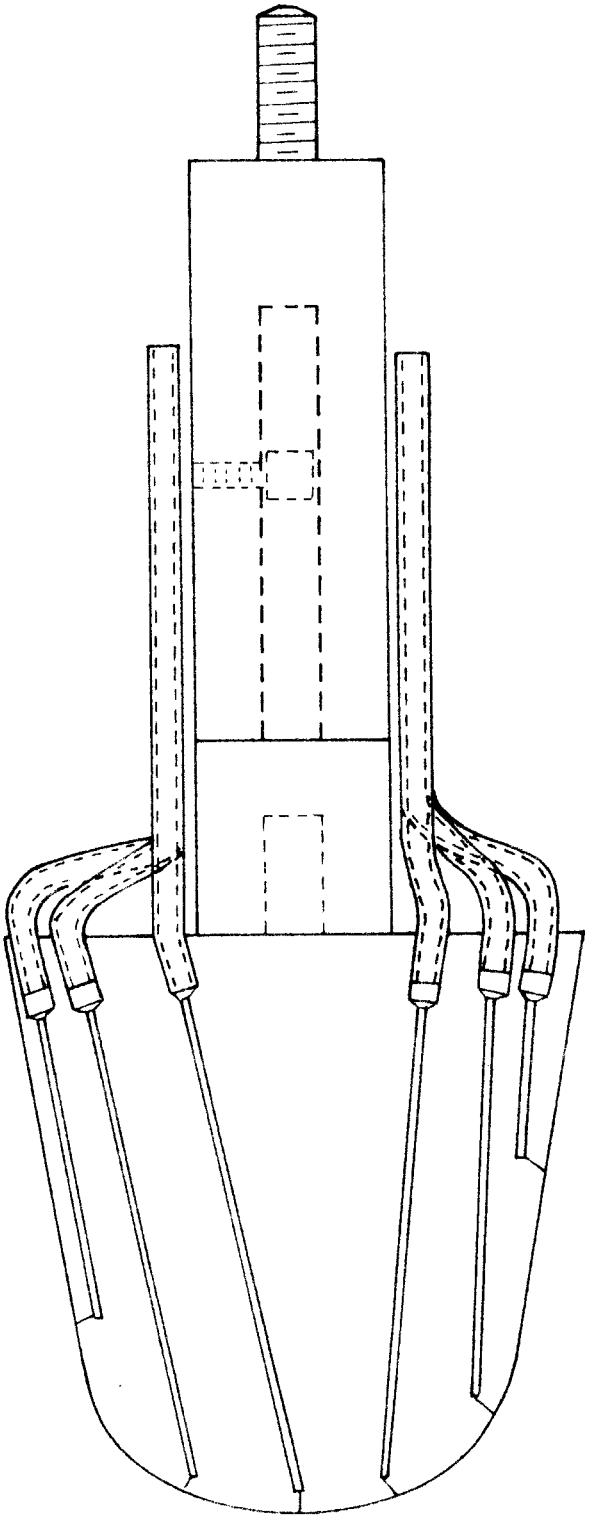

FIG. 4

DETAILS OF PRESSURE MODEL CONSTRUCTION

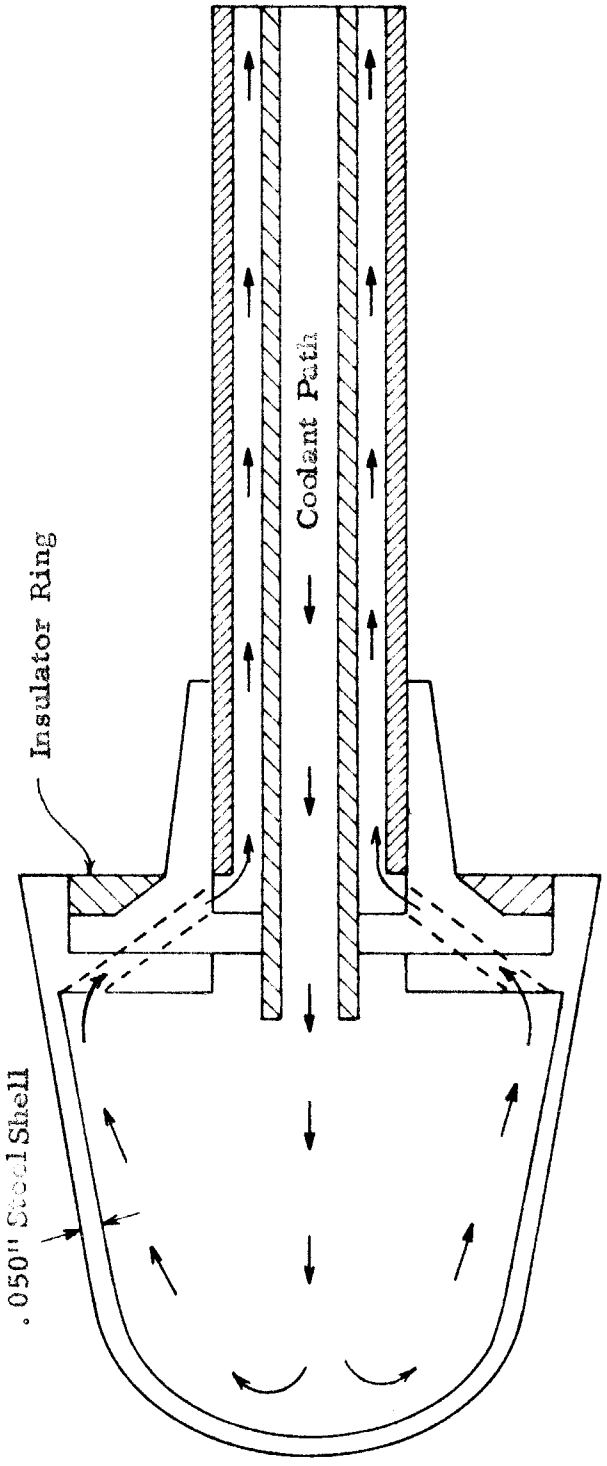

FIG. 5

DETAILS OF HEAT MODEL CONSTRUCTION

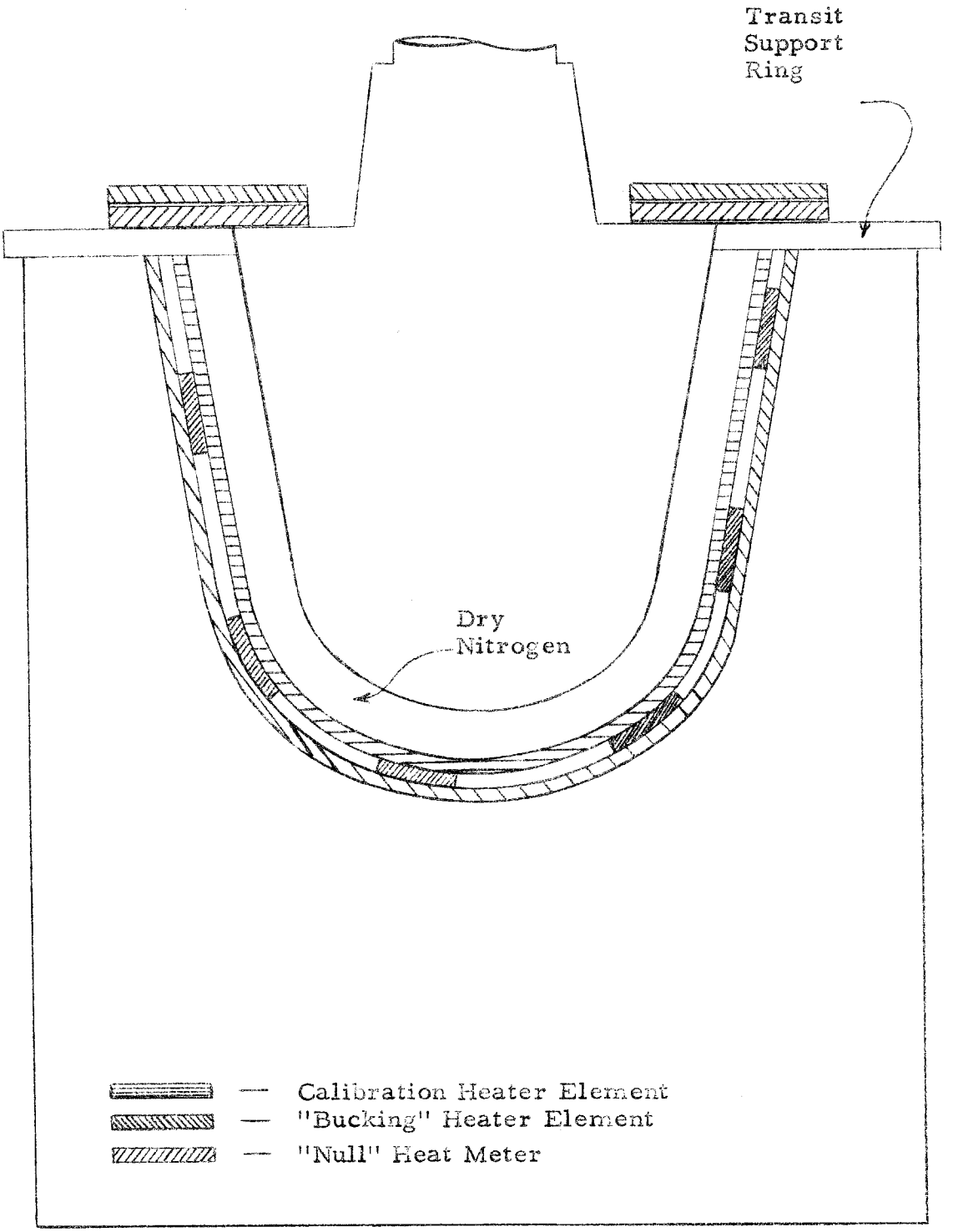

FIG. 6

DETAILS OF CALIBRATION OVEN

Orifice	S/D
1	.000
2	.083
3	.126
4	.169
5	.209
6	.264
7	.319
8	.373
9	.515
10	.651
11	.809
12	.957

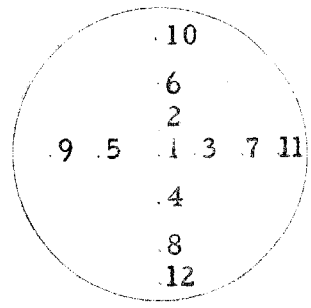

Pressure Orifices

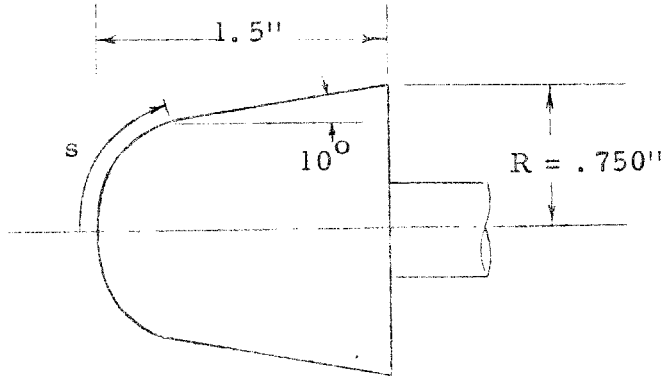

Heat Meter	S/D
1	.000
2	.074
3	.170
4	.264
5	.330
6	.446
7	.602
8	.775
9	.934

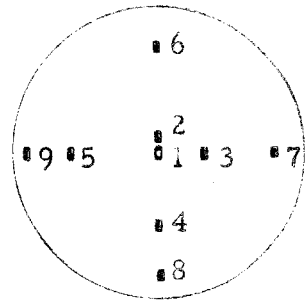

Heat Meters

FIG. 7

PRESSURE ORIFICE AND HEAT METER LOCATIONS

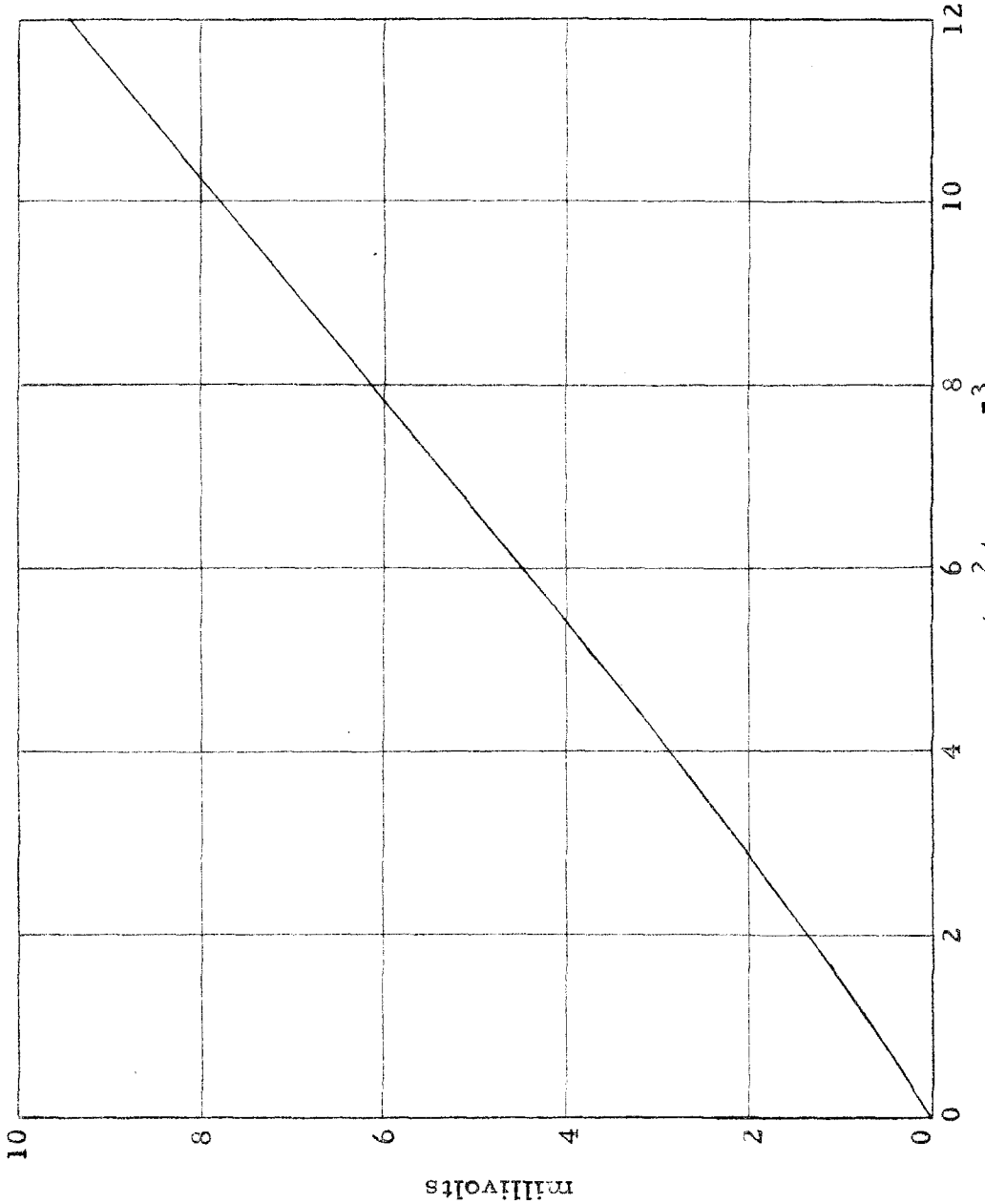

FIG. 8

TYPICAL HEAT METER CALIBRATION CURVE

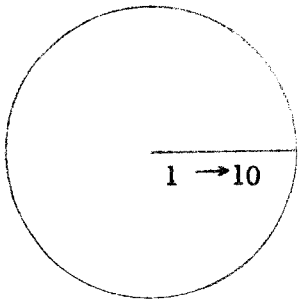

Line of Thermocouples

Thermocouple	S/D
1	.000
2	.0833
3	.167
4	.240
5	.350
6	.433
7	.527
8	.713
9	.847
10	.993

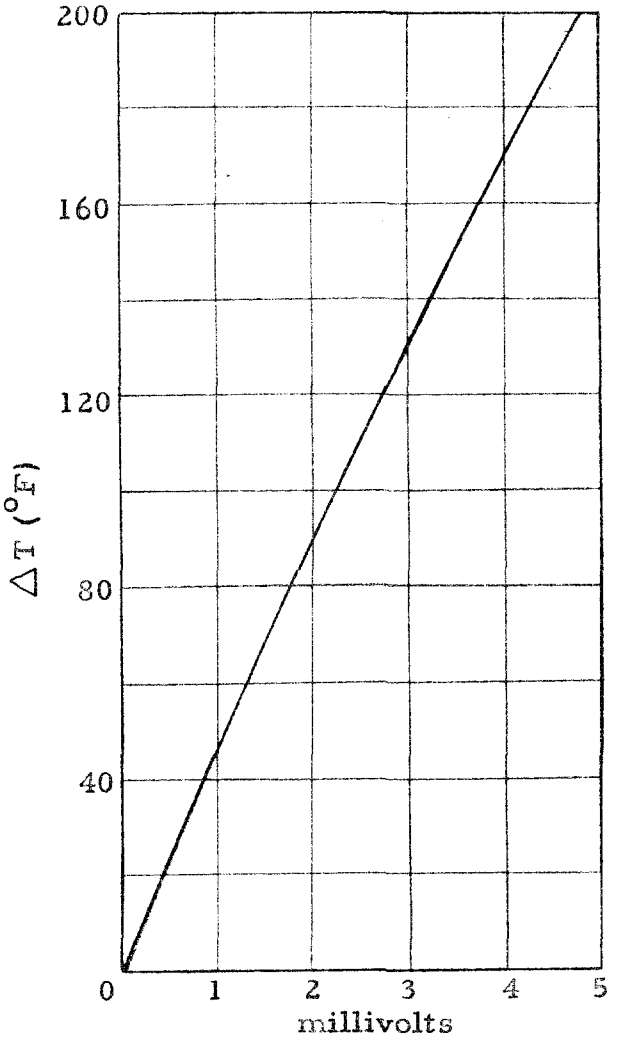

FIG. 9

SILVER-CONSTANTAN THERMOCOUPLE CALIBRATION CURVE AND THERMOCOUPLE LOCATIONS

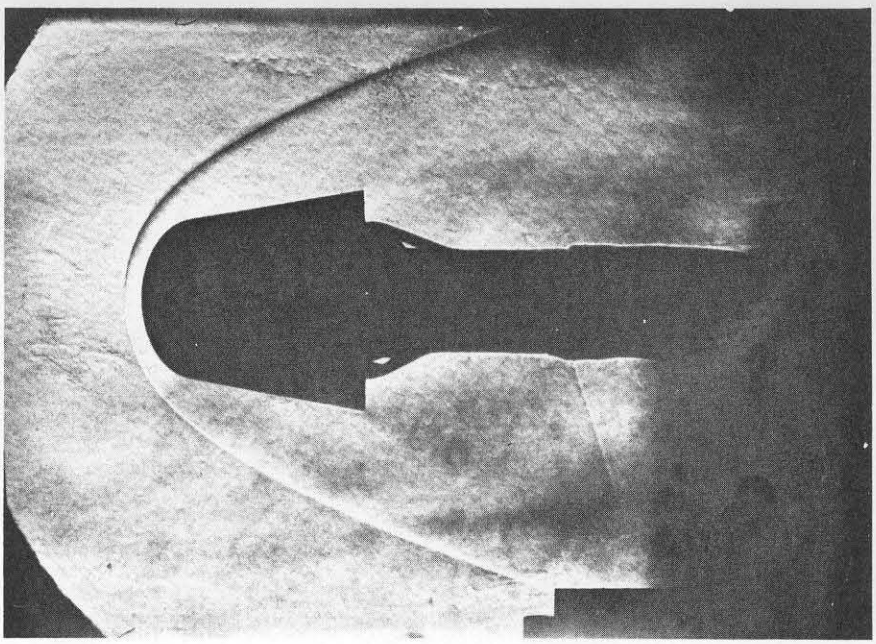

FIG. 10

SCHLIEREN PHOTOGRAPH OF PRESSURE MODEL

ANGLE OF YAW 0°, M = 5.8

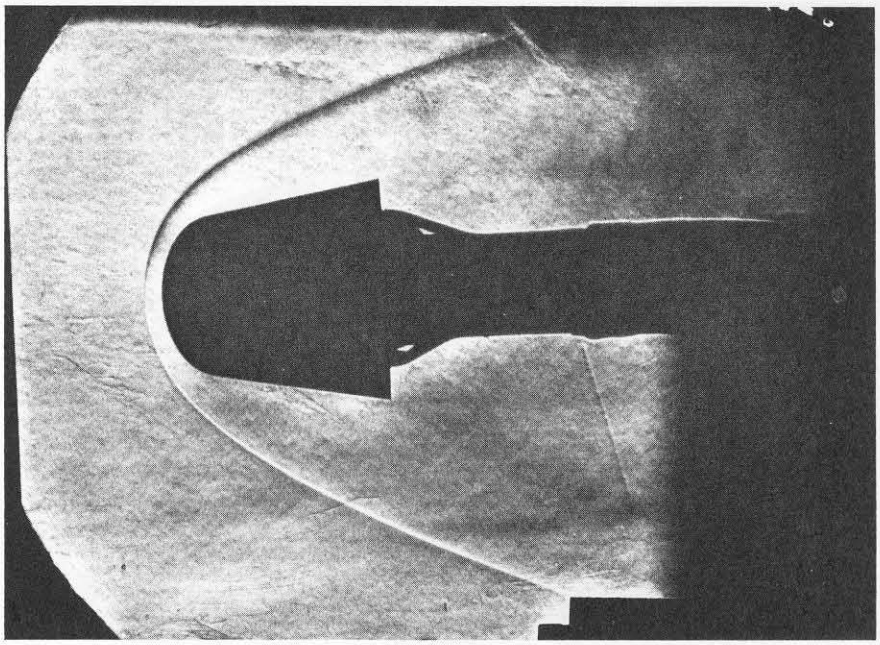

FIG. 11

SCHLIEREN PHOTOGRAPH OF PRESSURE MODEL

ANGLE OF YAW 4°, M = 5.8

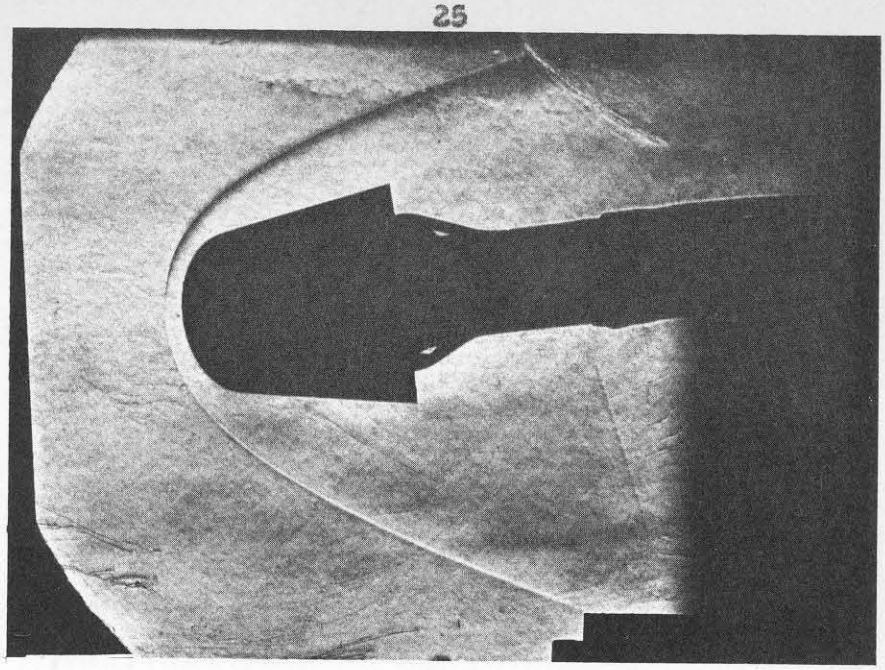

FIG. 12

SCHLIEREN PHOTOGRAPH OF PRESSURE MODEL

ANGLE OF YAW 8^{o}, M = 5.8

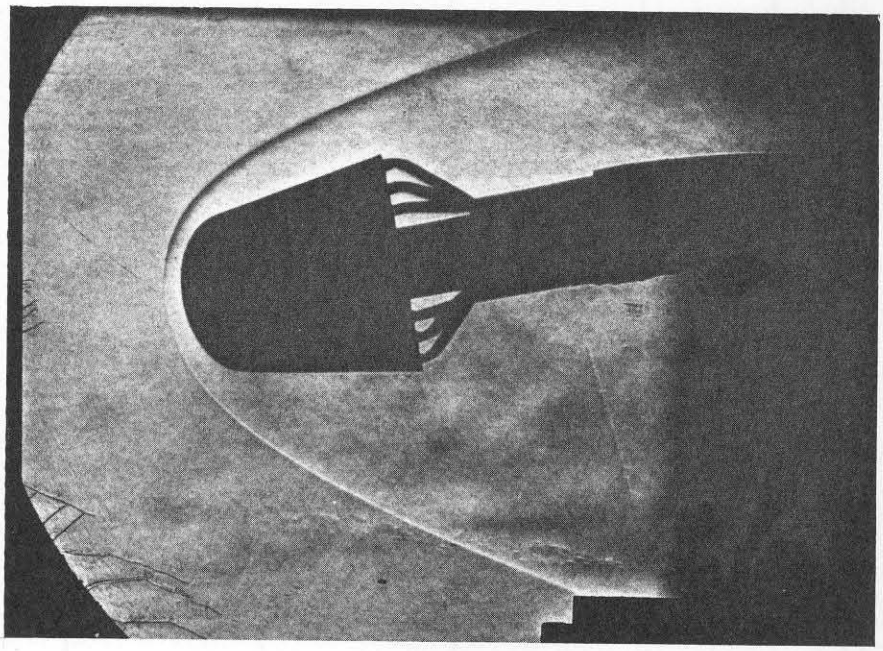

FIG. 13

SCHLIEREN PHOTOGRAPH OF PRESSURE MODEL

ANGLE OF YAW 12^{o}, M = 5.8

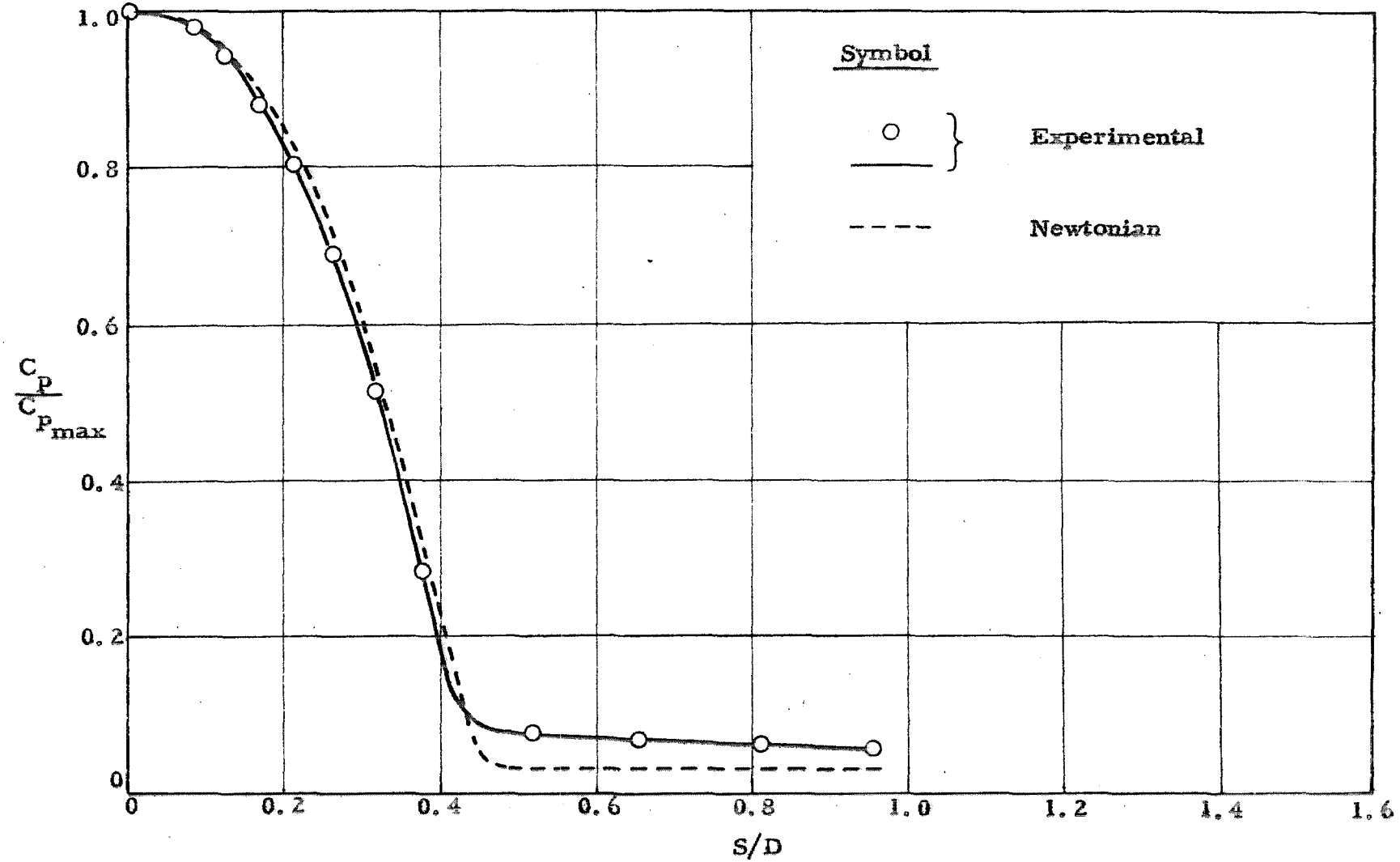

FIG. 14

SURFACE PRESSURE DISTRIBUTION, $\alpha = 0^{\circ}$

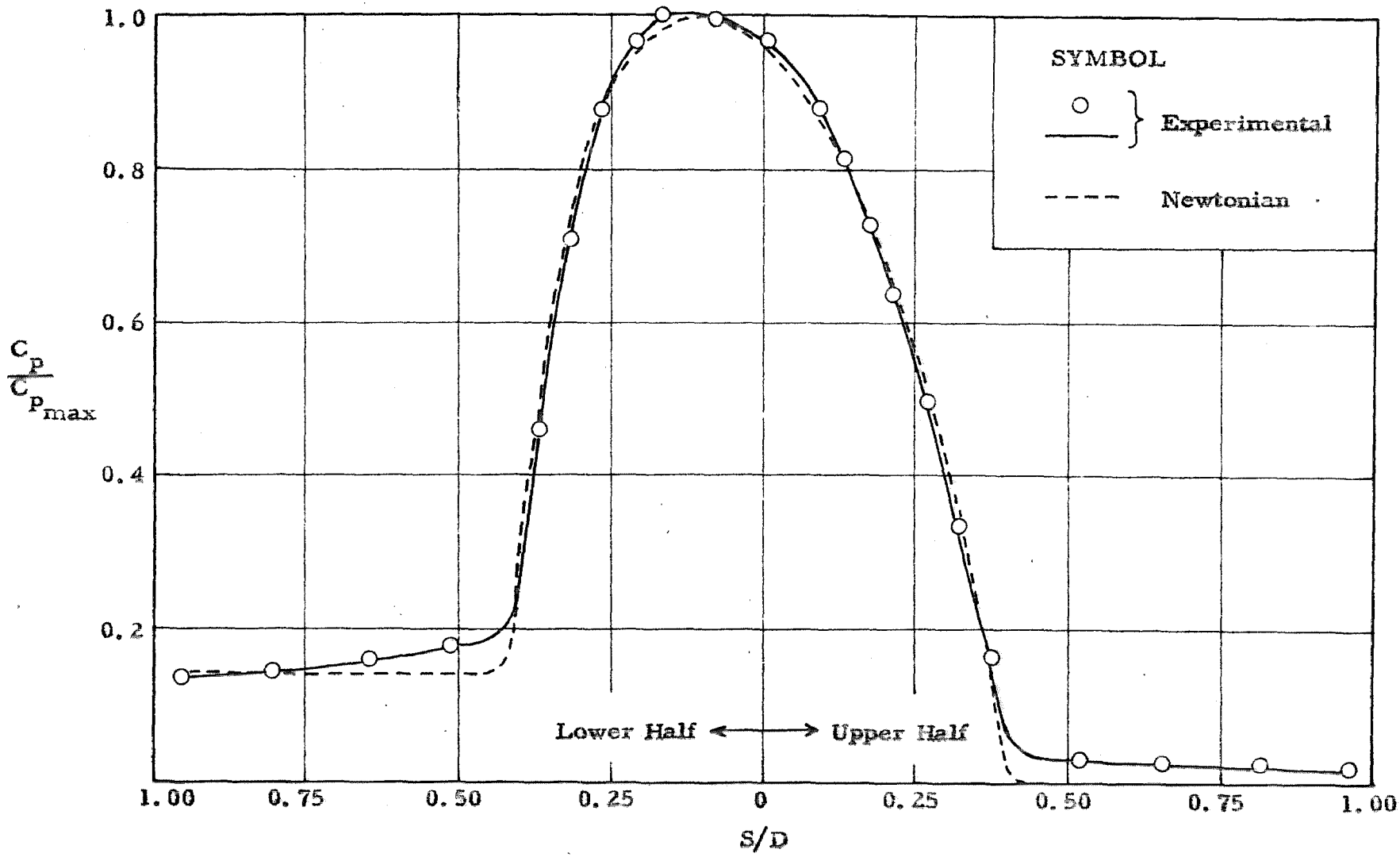

FIG. 15

SURFACE PRESSURE, VERTICAL MERIDIAN PLANE, $\alpha = 12°$

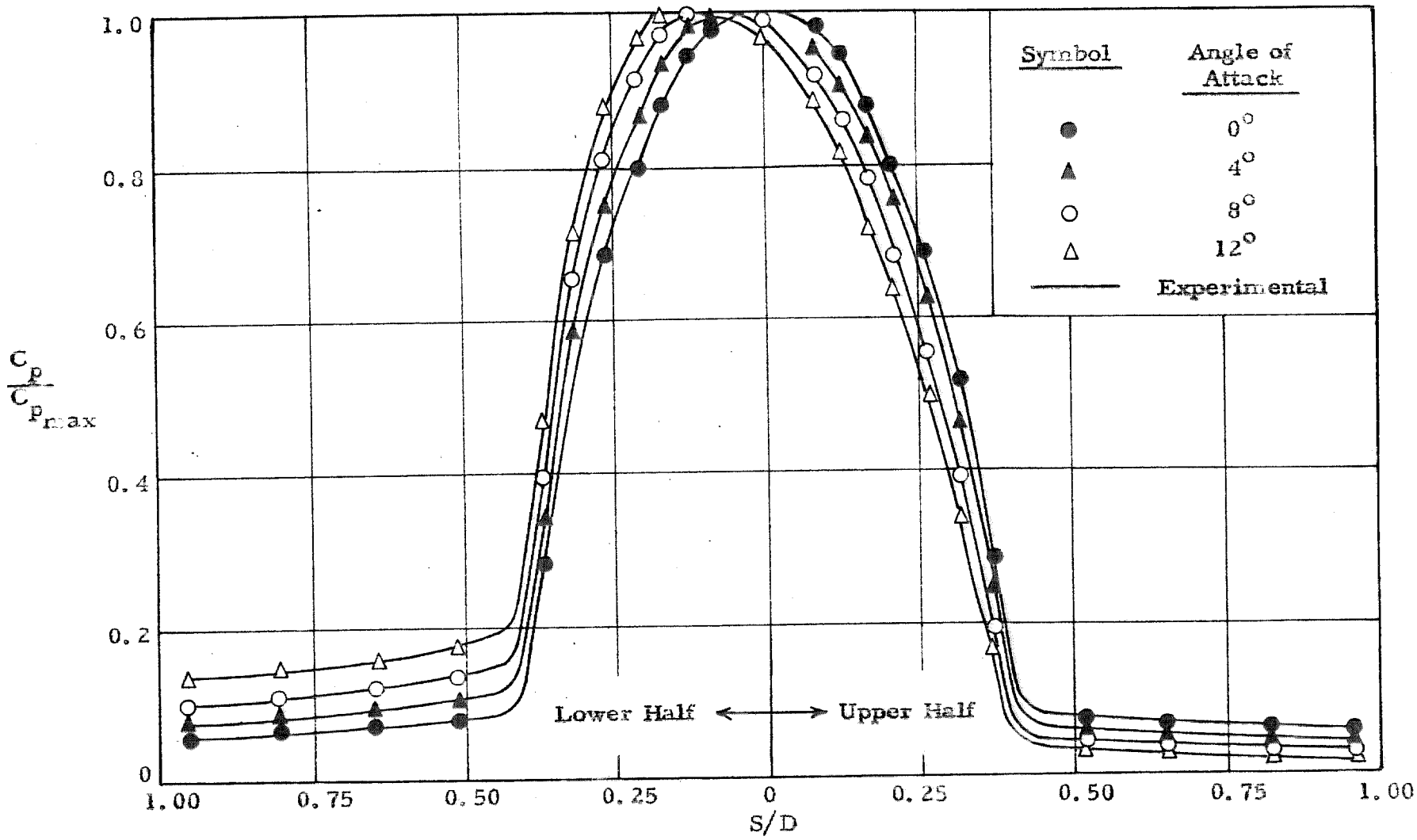

FIG. 16

SURFACE PRESSURE, VERTICAL MERIDIAN PLANE, $\alpha = 0$, 4°, 8°, 12°

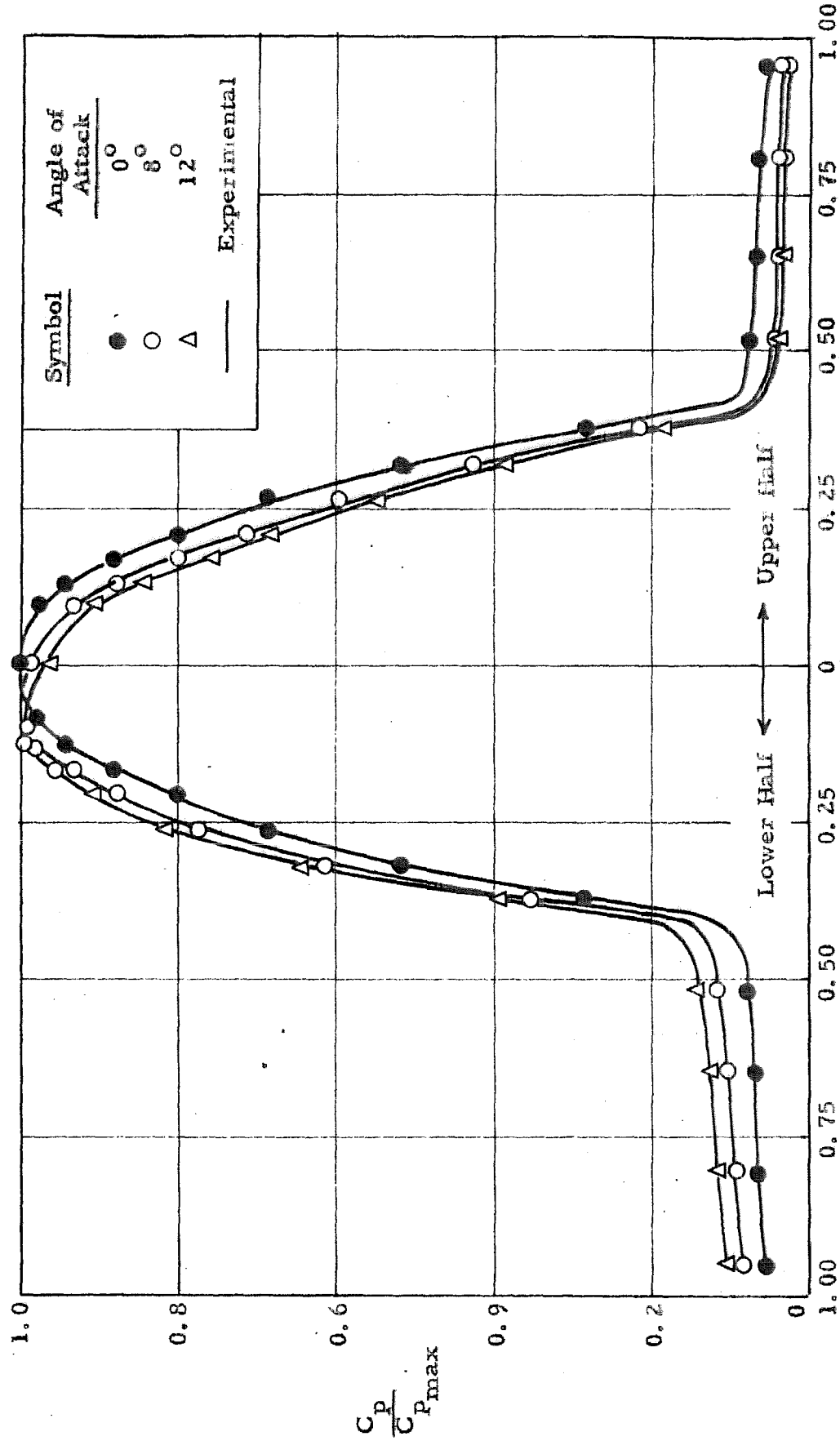

FIG. 17

SURFACE PRESSURE, DIAGONAL MERIDIAN PLANE, $\alpha = 0°, 8°, 12°$

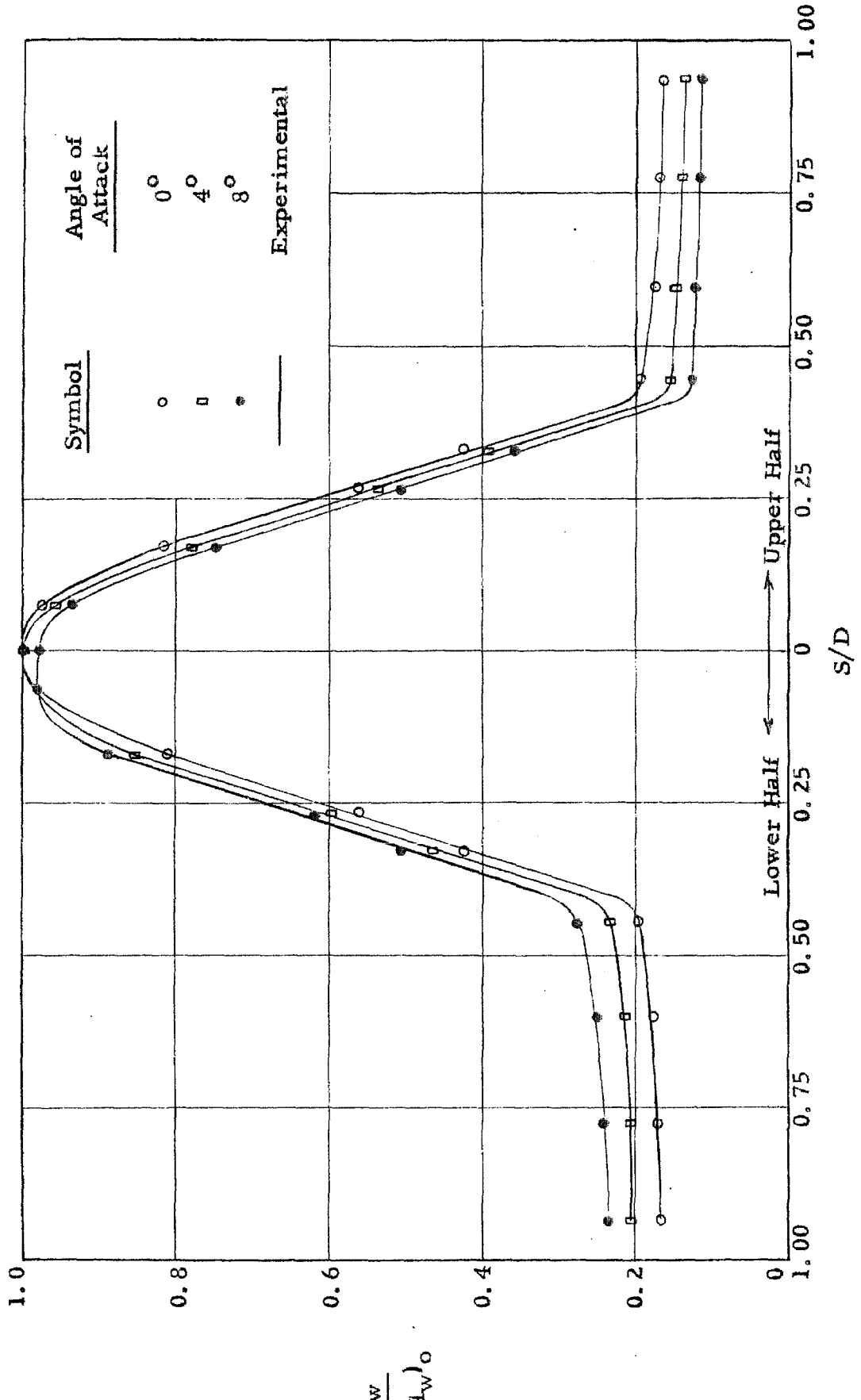

FIG. 13

HEAT TRANSFER RATE DISTRIBUTION, VERTICAL MERIDIAN PLANE, $\alpha = 0°, 4°, 8°$

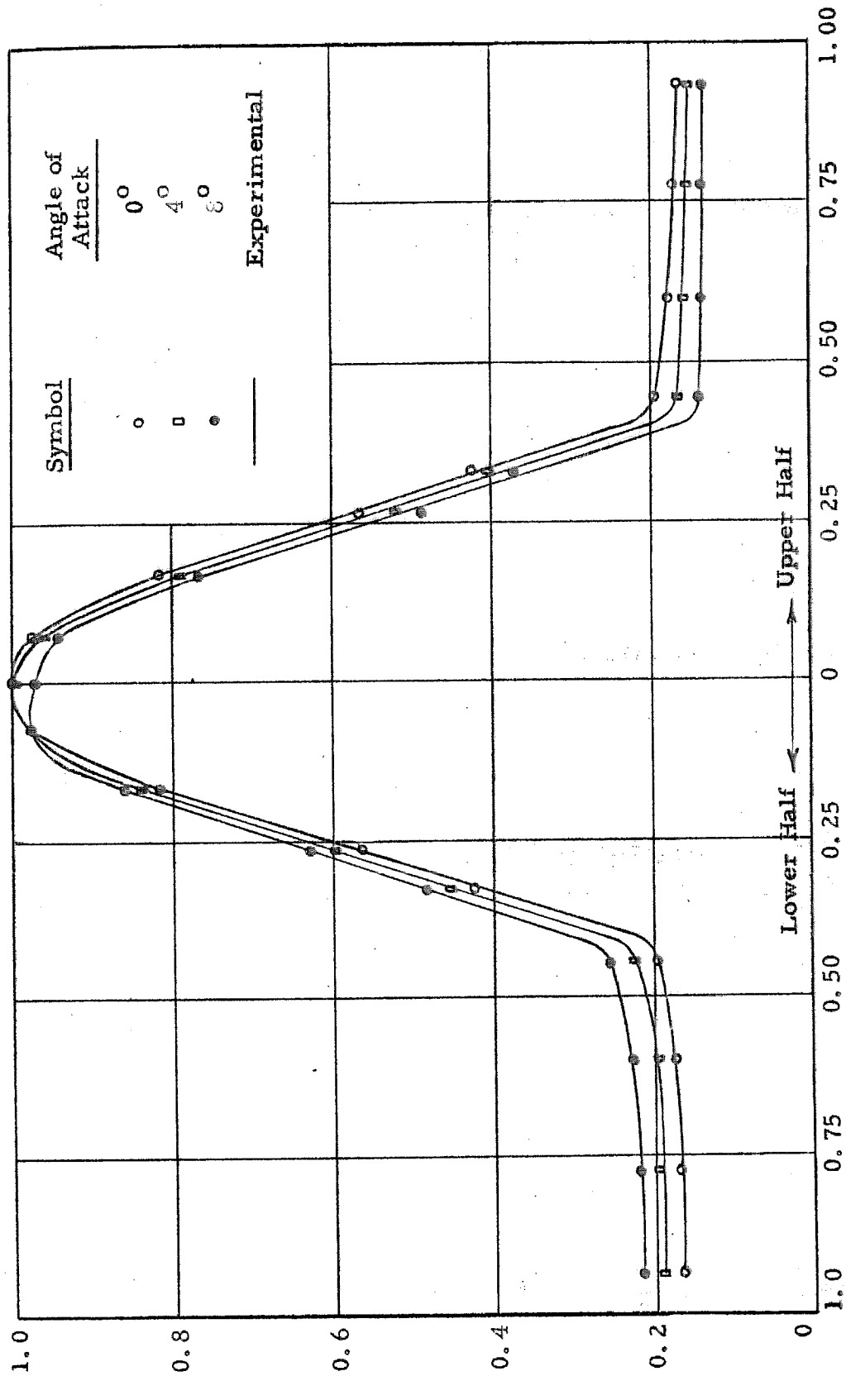

FIG. 19

HEAT TRANSFER RATE DISTRIBUTION, DIAGONAL MERIDIAN PLANE, $\alpha = 0°, 4°, 8°$

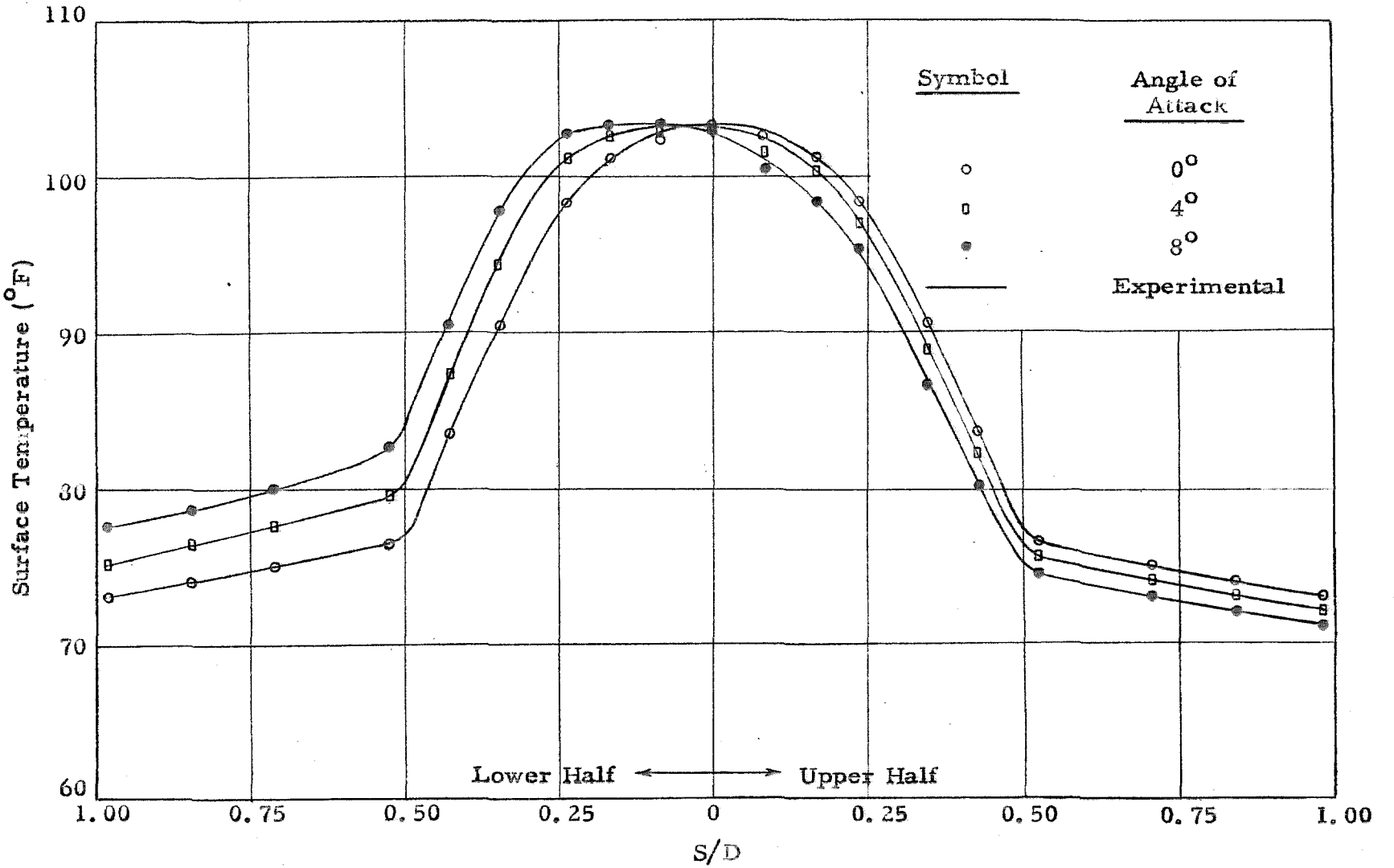

FIG. 20

SURFACE TEMPERATURE DISTRIBUTION, VERTICAL MERIDIAN PLANE, $\alpha = 0^{\circ}, 4^{\circ}, 8^{\circ}$

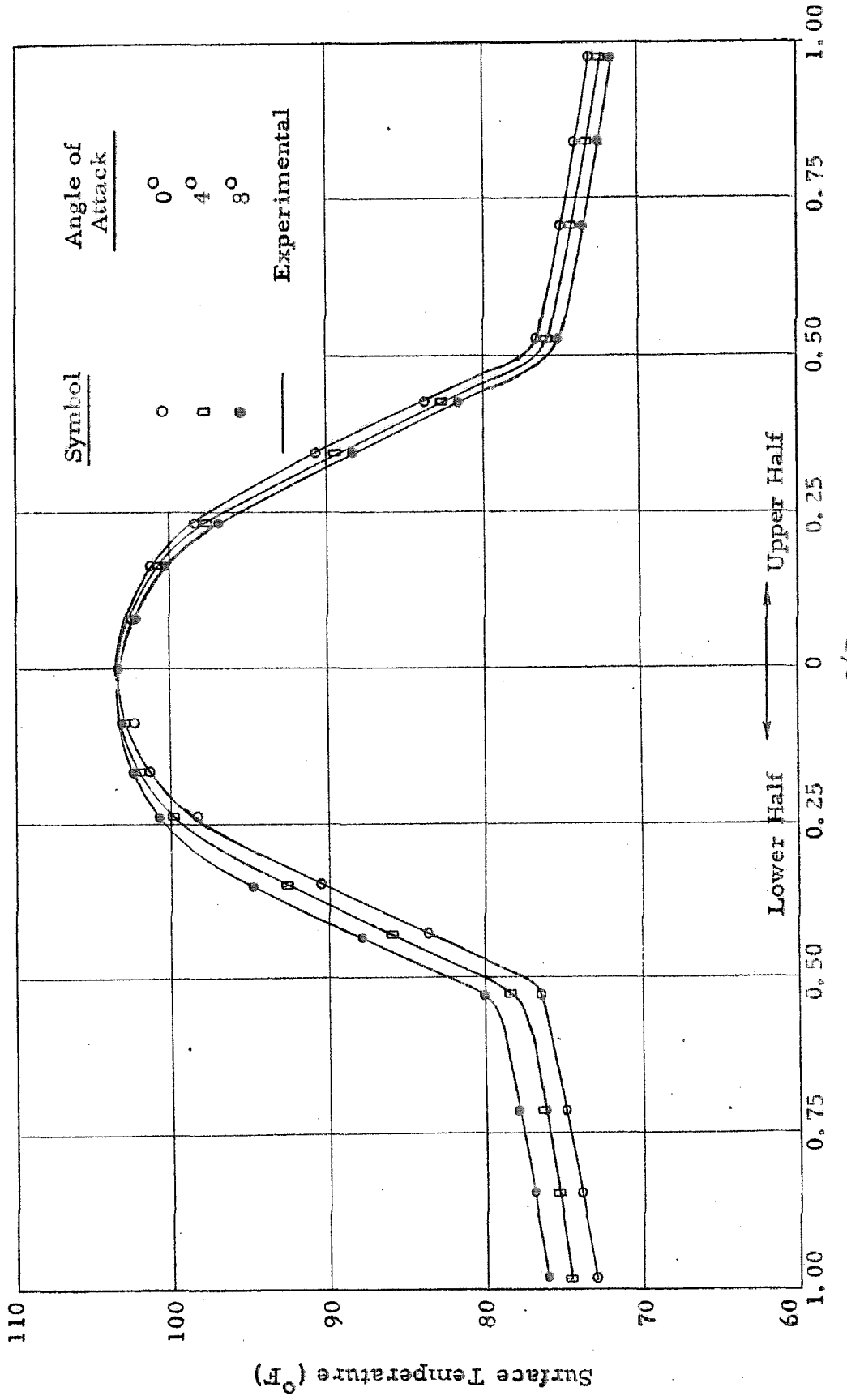

FIG. 21

SURFACE TEMPERATURE DISTRIBUTION, DIAGONAL MERIDIAN PLANE, $\alpha = 0°, 4°, 8°$